NONLINEAR FINITE ELEMENT EVALUATION OF THE STRUCTURAL RESPONSE TO LATERAL ACCELERATIONS OF THE ADOBE CHURCH OF ANDAHUAYLILLAS, PERU

Yue Wang[1], Zhi Qiao[1], Yumeng Dong[1], Carolina Briceño[2], Rafael Aguilar[2, *], Renato Perucchio[1]
[1] Department of Mechanical Engineering, University of Rochester, Rochester, NY, United States
[2] Engineering Department, Civil Engineering Division, Pontificia Universidad Católica del Perú – PUCP, Lima, Perú.

ABSTRACT

The Saint Peter Apostle church of Andahuaylillas was built at the early 17th Century and is a representative example of colonial adobe churches in the Andes. Although it has been subjected to constant aesthetic restoration in the recent years, a complete study of its seismic behavior is needed due to the brittle condition of its structural system (composed by a unfired-clay-bricks and earthen mortar known as adobe masonry) and its location in a region with high seismic hazard. This work is part of the integral seismic assessment of the building and focuses on the seismic evaluation of the triumphal arch by means of a static nonlinear analysis. For this purpose, nonlinear finite element (FE) models of the arch were implemented in Abaqus/CAE Explicit and TNO Diana considering a damage-plasticity formulation and a total-strain crack constitutive relationship, respectively, for representing the adobe quasi-brittle behavior. Following an analysis approach simulating up to complete structural collapse, the FE models were used to identify the critical accelerations leading to collapse and the damage patterns. A sensitivity analysis was also carried out considering different material properties for determining the influence of these parameters in the lateral capacity of the studied sub-structure. In addition, different geometrical conditions were considered to increase the capacity of the triumphal arch. Removing the window openings from sidewalls provided more capacity and different crack patterns. Heightening the sidewalls also had a significant influence on capacity.

KEYWORDS

Triumphal arch, pushover analysis, adobe masonry, FEM nonlinear explicit analysis.

INTRODUCTION

Adobe has been employed as a construction material around the world since remote times (Houben *et al*. 1994). In Peru, adobe bricks have been frequently used for the construction of churches, mainly during the baroque period in the Andean region. In the region of Cusco, along the so-called Andean baroque route – Figure 1(a), there are several adobe churches belonging to the baroque artistic movement. St. Peter Apostle of Andahuaylillas is the most important monument in this route. Figure 1(b) offers a view of the façade of the monument.

Over the last sixty years, the interest on the preservation of historic masonry buildings has been steadily increasing (Giuffrè and Carocci 1996). Numerous studies and interventions have substantially increased our knowledge of materials and construction processes. In particular, non-destructive diagnostic techniques have been developed in order to determine the current state of a structure of high cultural and architectural value without affecting its integrity. This diagnostic step is necessary prior to any intervention, because the effects of the intervention itself are difficult to predict and could negatively impact the stability of the structure.

Modeling and analyzing masonry structures are inherently difficult tasks and their complexity increases in the particular case of historical constructions. In order to carry out a structural evaluation, detailed information related to the construction history and architectural evolution must be acquired together with the geometry, fracture patterns and any other anomalies present in the structure. In addition, detailed knowledge of the building materials and their mechanical properties are essential for a proper execution of the evaluation (Binda and Saisi 2001). The necessary information is acquired through qualitative and quantitative research procedures involving the collection of data from preliminary studies in-situ and laboratory tests. These data will determine the type of structural analysis that needs to be applied to evaluate the monument.

(a)

(b)

Figure 1. St. Peter Apostle Church of Andahuaylillas: (a) location on the Andean baroque route and (b) façade (looking east)

In the case of masonry churches, several studies have focused on the assessment of the triumphal arch considered as a separate substructure. Mele *et al*. (2003) analyzed the Saint Ippolisto Martire church located in Southern Italy by means of kinematic limit and pushover analysis, aiming to assess the structural behavior and the seismic vulnerability. Since this construction consists of well-defined structural elements - such as the façade, triumphal arch, lateral walls, etc.- the separate study of individual elements provides information on the global structural performance as well as useful indications of the effectiveness of specific intervention measures on the element in question. Three specific elements of the church were studied carrying out a simplified assessment of the seismic behavior: chancel end wall, triumphal arch and a longitudinal section of the nave arcade. In the case of the triumphal arch, a high correlation was obtained between limit and pushover FEM analysis results, indicating a maximum capacity of 0.283g. Additionally, several analyses were performed on the arch to evaluate the effect of different values of the compressive and tensile strength.

Similarly, a simplified procedure for assessing the seismic capacity of masonry arches is proposed in De Luca *et al*. (2004). This involves kinematic limit analysis and linear static FEM analysis, the former aiming to determine the acceleration that promotes instability – and thus failure - of the assumed kinematic mechanism, the latter aiming to detect tensile and compressive stress zones which may produce the fractures and thus the mechanism. Nonlinear FEM analysis was used in order to verify the results of the limit analysis. Two triumphal arches from different churches were selected as case studies: the church of San Giovanni a Mare and the church of San Giovanni Maggiore both in Southern Italy. Each case presents particular architectural characters. The first triumphal arch has non-symmetrical shape, with a main semi-circular arch, flanked by two lower and narrower pointed arches. The second is a large semi-circular arch with very wide and stocky lateral walls.

The critical zones, and consequently the potential hinges, were determined due to these stress distributions computed via linear FEM analysis. As in the previous case, the critical collapse multiplier was defined by varying the position of the hinges. In both cases, as shown in Figure 3, a good correlation between the limit and nonlinear FEM results is obtained. The collapse multipliers from limit analysis were 0.224 and 0.4, and the maximum load capacities from nonlinear FEM were 0.20 and 0.31 for San Giovanni a Mare and San Giovanni Maggiore, respectively. Note that, despite the marked geometrical differences, a similar ‘global-type’ kinematic mechanism was assumed for both arches

Our paper presents a portion of a preliminary study of the seismic behavior of St. Peter Apostle Church of Andahuaylillas. The building, constructed almost entirely with adobe bricks and located in a region with major seismic activity, is in constant risk. Because the church is actively used, the people of the local parish are also at risk. In the following, the historical, architectural and structural aspects together with a detailed description of the triumphal arch of the church are provided. We then report the details of the dynamic tests carried out on the bell tower and of the subsequent FEM model calibration procedure followed to determine the elastic properties of the adobe bricks. Finally we discuss the pushover analysis performed to evaluate the influence of different structural elements on the capacity of the arch under in plane accelerations. To this aim, we use nonlinear FEM models developed in Abaqus/CAE Explicit and Diana.

SAINT PETER APOSTLE CHURCH OF ANDAHUAYLILLAS

St. Peter Apostle church is located in the main square of the village of Andahuaylillas. Although the main function of the church is religious, it also supports the village in economic and development programs (anadahuaylillas.com 2015). The church was built by Jesuits over a pre Columbian Huaca and, based on the

style of the paintings inside the church, its erection dates from the late 16th or early 17th century (Castillo *et al*. 2012). The building follows a west-east orientation and is composed of the nave, the presbytery, the bell tower and several side chapels, as shown in Figure 2(a). At the west front, the main nave connects to the baptistery, the bell tower, the choir loft, and two chapels. The presbytery is separated from the nave by the triumphal arch and opens on four side rooms. The second level of the church, which is accessed from the bell tower, consists of a choir loft and an open chapel.

The substructure under study is the triumphal arch, consisting of the arch proper with the tympanum and the lateral shear walls corresponding to the west walls of the side chapels. The 3D model in Figure 2(b) provides an architectural view of the substructure (in this case, including sections of the nave walls.) The triumphal arch is mainly composed by adobe and brick masonry, with an average thickness of 1.5m.

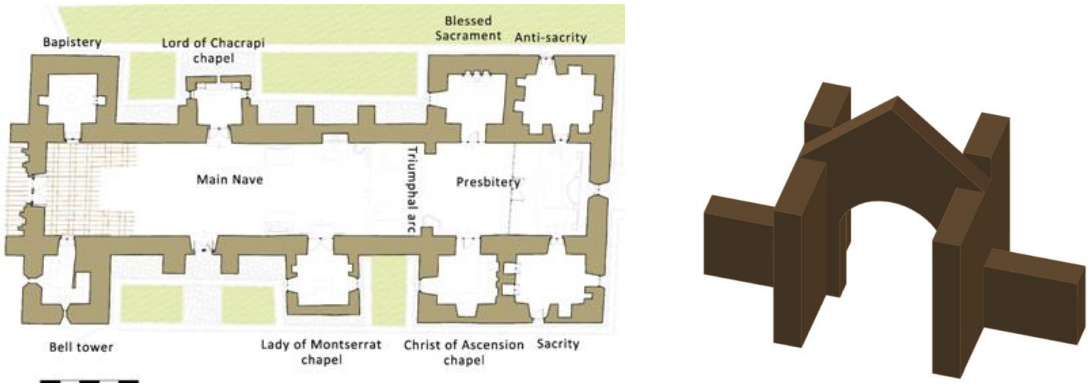

(a) (b)

Figure 2 Architectural representation: (a) Plan view of the church, and (b) 3D model of the triumphal arch

It is not possible to completely asses the deeper damage of the church accumulated over the years because the building has undergone conservation works in the last 50 years (Vargas *et al*. 2013). To complicate matters, the majority of the previous works were executed taking into account the aesthetic - and thus non-structural – aspects only. Deep fractures in the walls of the presbytery and the chapels, and in the triumphal arch have been identified. For example, a large fracture is observed in the south wall next to the triumphal arc and diagonal deep fissures are present in the tympanum above the triumphal arch, as shown in

Figure 3 Deep fissures on the triumphal arch of Andahuaylillas church

OPERATIONAL MODAL ANALYSIS AND DETERMINATION OF ELASTIC PROPERTIES

Ambient modal identification, also known as Operational Modal Analysis (OMA) (Aguilar *et al*. 2013 a), offers a useful approach to study earthen historical constructions through the identification of structural conditions, such as local damage (Fonseca and D'Ayala 2012, Aguilar et al 2013b). Being a non-destructive diagnosis technique, OMA is highly recommended for the application on historical constructions. As part of this preliminary study, OMA tests were carried out in the bell tower of the Andahuaylillas church in order to estimate the dynamic characteristics of the entire structure. Tests were performed in the tower in order to capture higher amplitude of the modal response. The resulting measurements were used to calibrate the accuracy of a global linear FEM model and thus determine the elastic properties of the adobe material, i.e., Young's modulus and Poisson ratio.

OMA tests in the bell tower were carried out by using the ambient noise as the excitation source. Eight measuring points according to a biaxial configuration were established in seven setups, considering two fixed and two routing sensors. The transducers used were four piezoelectric accelerometers with a sensitivity of 10 V/g and a dynamic range of ± 0.5 g together with an USB-powered 24 bits resolution data acquisition module. The data processing was carried out using the stochastic subspace identification method (SSI) implemented in the Artemis Software. The first three mode shapes identified are displayed in Figure 4.

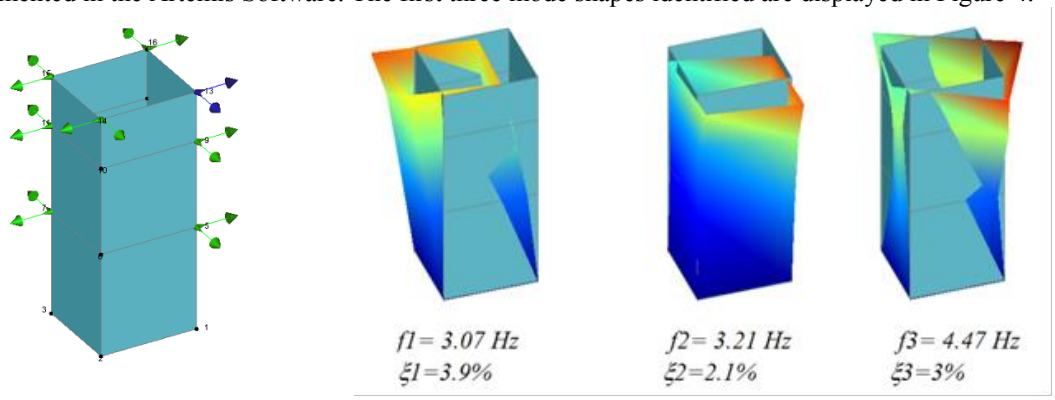

(a) (b)

Figure 4. Modal identification tests in the bell tower: (a) general test setup and (b) first three mode shapes

For the church, the model calibration is based on a modal analysis approach, for which the structural response is considered to remain in the elastic range. Two FEM models were built in Diana (2013) and Abaqus/CAE (2013). In both cases, the adobe masonry was represented as a homogeneous linear elastic material. The models were calibrated via a sensitivity analysis of the material properties and boundary conditions, by comparing the results of FE modal eigenvalue analysis to those of the OMA experimental tests. Modal Assurance Criterion (MAC) (Allemang 2003) was used to compare the experimental and numerical mode shapes and frequencies. At the end of the calibration process, a high correlation is observed between the numerical model and experimental results from both models. The first three modes shapes have MAC values of 0.95, 0.97 and 0.75, respectively. The final elastic properties of materials were assumed based on the recommendations given in (Fonseca and D'Ayala 2012, NTE.010 2006). The elastic properties resulting from the calibration process are presented Table 1.

Table 1 Elastic properties of materials

Material	Specific weight, w (KN/m^3)	Young's modulus, E (MPa)	Poisson ratio, ν
Adobe masonry	15.1	350	0.25
Rubble stone masonry	24.0	800	0.20
Wooden elements	4.7	10,000	0.20

PUSHOVER ANALYSIS

Pushover analysis has been developed as an acceptable approach for assessing the damage sequence due to seismic action. The analysis is helpful to evaluate the performance of buildings through displacement verifications, to identify critical zones in order to proceed with local implicit safety verifications, and to analyze the effects of seismic retrofitting. In this study a series of geometrical models developed in Abaqus/CAE Explicit and Diana were used to evaluate the influence of structural elements on the lateral capacity and on the damage pattern of the triumphal arch.

In Abaqus/CAE Explicit adobe was modeled as a quasi-brittle material using the concrete damaged plasticity formulation. In order to evaluate the sensitivity of the structural response to the tensile and compressive fracture energy three nonlinear material models were constructed. All have the same tensile and compressive strength, but two different sets of fracture energies were used to represent the nonlinear softening behavior in tension and compression. The first set of nonlinear material properties was extrapolated from the experimental results given in the previous section following recommended procedures for masonry material given in the literature (Van der Pluijm 1999, Lourenço 2009). The compressive strength was taken as fm = E/400, where E is 350 MPa, and thus fm = 0.875 MPa. The tensile strength and the tensile fracture energy were estimated as $ft = fm/10$= 0.0875

MPa and Gf = 4 Nm^{-1}, respectively. Assuming a ductility factor of 1.6 mm (Lourenço 2009), the compressive fracture energy was estimated as Gm=1.6 x fm= 1,400 Nm^{-1}. Following the masonry models by Lourenço (2009) the compression curve is parabolic while the tension softening is represented by an exponential decay. Taking into account that the characteristic length of our FE models is h = 0.207 m, the compressive and tensile stress versus plastic strain curves shown in Figure 5 are generated.

For constructing the second set of nonlinear material properties we fitted to our case the tensile and compressive stress versus plastic strain curves adopted by Tarque et al. (2010) for an adobe Abaqus model. In this case, too, the compression curve is parabolic while the tension softening is represented by an exponential decay. We scaled these curves so that the strengths in tension and compression match 0.0875 MPa and 0.875 MPa, respectively. For h = 0.207 m the corresponding tensile fracture energy for this material model is Gf = 32 Nm^{-1} while the compressive fracture energy is Gm = 550 Nm^{-1}. The compressive and tensile stress versus plastic strain curves are shown in Figure 5.

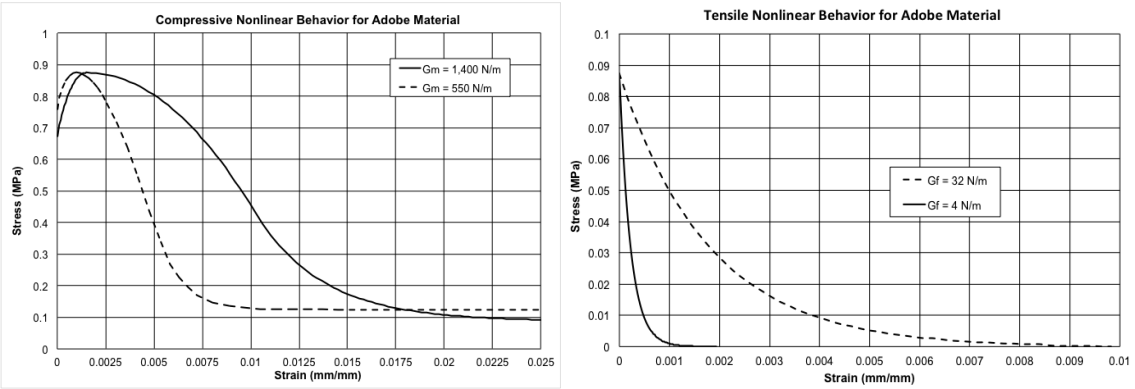

Figure 5. Constitutive laws for constructing the material models in Abaqus/CAE Explicit

The three material models used in Abaqus/CAE Explicit are given in Table 2. As noted earlier, all materials have the same tensile and compressive strengths, but Material 1 is characterized by high tensile fracture energy and low compressive fracture energy, while the opposite is true for Material 3. Material 2 combines low fracture energies for both tension and compression.

Table 2 Material models used in Abaqus/CAE Explicit

Material model	Compressive fracture energy Gm [N/m]	Tensile fracture energy Gf [N/m]
1	550	32
2	550	4
3	1,400	4

The elastic and the general plastic properties common to all three material models used in Abaqus/CAE Explicit are presented in Table 3 and 4, respectively.

Table 3 Elastic properties of adobe masonry in Abaqus/CAE Explicit and Diana

Specific weight (kN/m^3)	E (MPa)	ν
15.1	350	0.25

Table 4 Plastic properties of adobe masonry in Abaqus/CAE Explicit

Dilation Angle	Eccentricity	fb0/fc0	K Parameter	Viscosity Parameter	Compressive strength (MPa)	Tensile strength (MPa)
1	0.1	1.16	0.6666	1E-8	0.875	0.0875

In Diana the non-linear behavior of the masonry was modeled by the adoption of a constitutive relationship based on the total strain crack model, which provides good stability in the opening crack control, as well as moderate computer cost. The material laws in compression and tension were assumed to follow parabolic and exponential laws, respectively (Lourenço 2009). Figure 6 shows the compressive and tensile curves used to

represent the adobe masonry. Post-cracked shear behavior was modeled using a shear retention factor of 0.01. Similarly to Abaqus/CAE models, the compressive and tensile strength were 0.875 MPa and 0.0875 MPa, respectively. The fracture energy was 1,400 Nm^{-1} in compression and 4 Nm^{-1}in tension. The elastic properties are identical to those adopted for the Abaqus/CAE models – see Table 3.

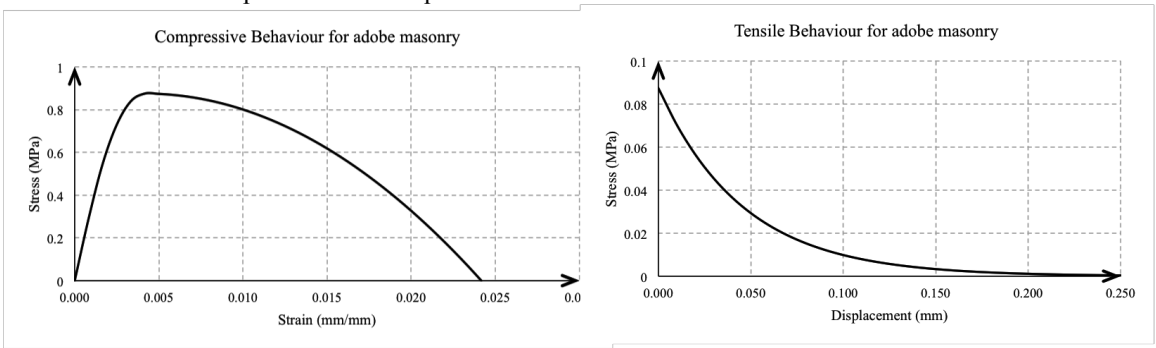

Figure 6. Nonlinear material behavior for Diana models

The Abaqus/CAE Explicit analysis was articulated in three loading steps. The kinematic boundary conditions were set in the initial step. To simulate a realistic situation, gravitational acceleration was applied first, followed by the horizontal acceleration load. Both accelerations were applied as uniform fields acting at each element integration point of the entire model. The intensity of each field was set to increase linearly with time. In order to force the explicit dynamic to simulate quasi-static conditions during loading, the maximum time increment for each step was set to $1.x10^{-6}$. In a similar fashion, constant gravity loads in Diana models were applied to each case under study. Subsequently, the structure was pushed laterally with a horizontal acceleration ramp loading applied uniformly over the entire mesh. The regular Newton–Raphson method combined with the arc-length procedure was adopted in order to determine the solution of the nonlinear problem.

The triumphal arch is composed of several sub-structural elements: the arch proper, the tympanum, and the sidewalls (here considered with and without window openings.) Each element contributes distinctively to modulating the capacity of the triumphal arch and therefore must be examined through a separate FEM model. Four structural models are reported in the present study: M1, the arch proper; M2, the arch with the tympanum only; M3, the arch including the tympanum and the lateral walls without windows, and M4, the same configuration as M3 but with the addition of window openings. Each model was analyzed in Abaqus/CAE Explicit and Diana using nearly identical 2D meshes of quadratic triangular plane stress elements - CPS6 and CT12M, respectively. All models were fully constrained on their bottom edge. Finally, we used Models 5 and 6 to explore how the height of the lateral walls affects the capacity of Models 3 and 4, respectively.

RESULTS

Model M1: the Arch

Figure 7 (a) shows the capacity curves for Model M1 calculated for the top left corner by Abaqus/CAE with Materials 1-3 and by Diana. Figure 7 (b) shows the damaged status of the model at the computed collapse conditions in Abaqus in terms of maximum principal plastic strains. A similar picture in terms of element damage status is computed in Diana. As expected, the damage originates at the center of the intrados at the end of gravity loading, indicating that a vertical crack begins forming in this zone. When horizontal acceleration is applied, the crack is deviated laterally and then downward. As shown in Figure 7 (b) two additional tensile fractures occur at the top right shoulder and at the bottom of the right pier. As a result, the right pier gradually separates from the arch and ultimately collapses through rotation, while the arch itself breaks into two separate parts. Immediately thereafter the left pier also collapses after developing a fissure at the springing of the arch. The damage at the right bottom corner of the right pier is due to the high compressive stresses produced at impending rotation. From a kinematic perspective, the location of the hinge about which the pier is rotating depends upon the compressive strength of the material.

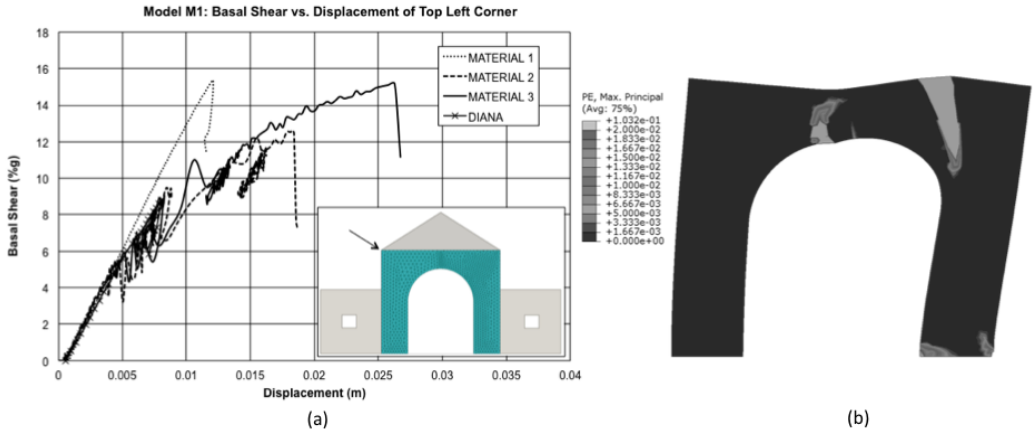

Figure 7 (a) Capacity curves for model M1, and (b) maximum plastic strains at collapse (Abaqus/CAE); displacements are computed at top left corner indicated by arrow in (a)

Material 1 produces a capacity of 15%g with a nearly linear response up to collapse. Reducing the tensile fracture energy – Material 2 – lowers the capacity to 12.3%g and results in a markedly nonlinear behavior, which could be attributed to the right pier separating more easily from the arch. With Material 3 the compressive fracture energy increases, thus increasing the resistance to damage at the right bottom corner of the critical right pier. The capacity grows back to almost 15%g but the ductility increases two and a half times with respect to Material 1. Diana produces similar results to Material 2 and 3, but terminates at approximately at 9%g.

Model M2: the Arch with Tympanum

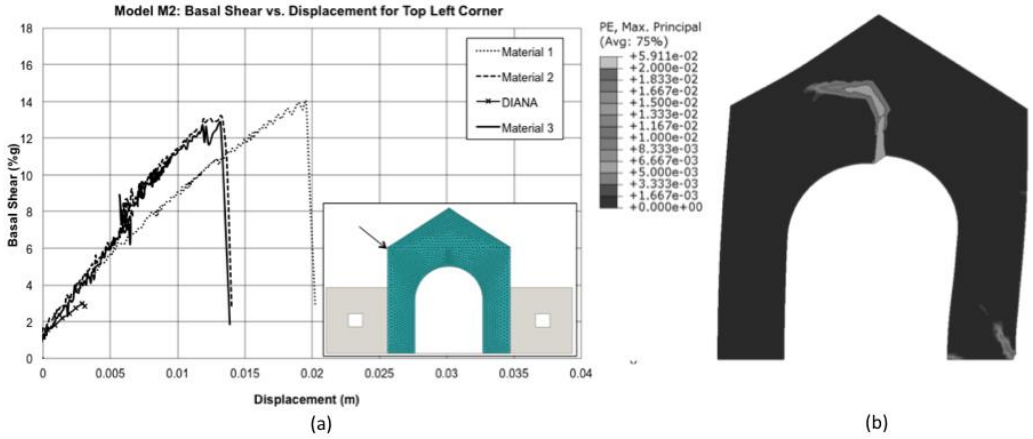

Figure 8 (a) Capacity curves for model M2, and (b) maximum plastic strains at collapse (Abaqus/CAE); displacements are computed at top left corner indicated by arrow in (a)

Figure 8 shows the capacity curves for Model M2 and the damage status of the model at the computed collapse conditions in terms of maximum principal plastic strains. As for M1, a vertical crack forms at the center of the intrados at the end of gravity loading, and then grows laterally with the horizontal acceleration being applied. However, there is no pier rotation in this case. Rather, collapse appears to be triggered by a shear fracture developing diagonally in the right pier before the center crack reaches the extrados. The reduction in tensile fracture energy in Material 2 and 3 compared to Material 1 affects the capacity only by 7%. Diana results stop at only 3%g.

Model M3: the Arch with Tympanum and Lateral Walls

The capacity curves for Model M3 and the damage status at collapse are illustrated in Figure 9. Contrary to the previous case, due to the constraining effect of the lateral walls on the downward deformations induced by gravity, gravitational loading produces no damage at the center of the intrados or elsewhere in the structure.

Under horizontal accelerations increasing linearly from 0 to 0.6 g an asymmetric crack starts from the intrados of the arch and proceeds laterally followed by a fissure separating the left wall from the left pier. For Material 1, the collapse is due to the separation of the left pier followed immediately by a shear fracture of the right wall - see Figure 9 (b). The capacity curve reaches 53%g – 3.5 times the capacity of Model 1.

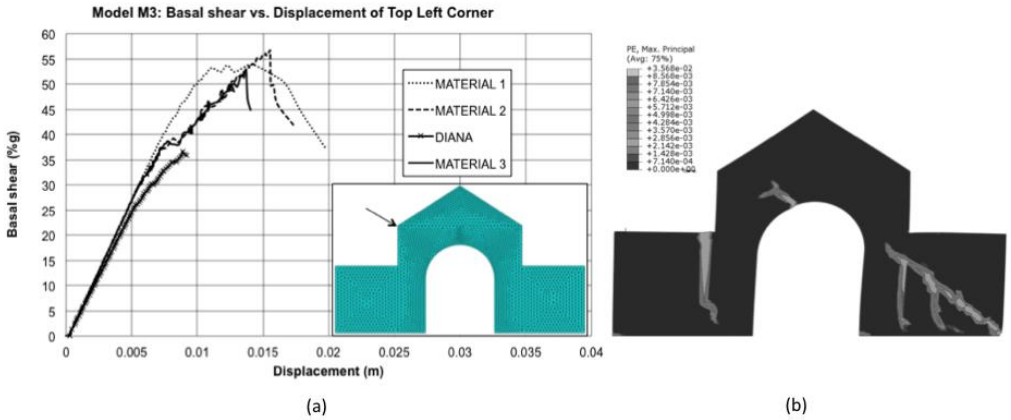

Figure 9 (a) Capacity curves for model M3, and (b) maximum plastic strains at collapse (Abaqus/CAE); displacements are computed at top left corner indicated by arrow in (a)

The failure picture for Materials 2 and 3 is more complex. The crack at the intrados of the arch turns downward and produces the detachment of a section of the arch at 45%g basal shear. This constitutes only a partial collapse and the structure continues to resist up to 56%g, for Material 2 and 53%g for Material 3. The increased compressive fracture energy in Material 3 appears to facilitate the formation of a shear fracture in the right lateral wall. Diana' s results show a good correlation in terms of stiffness, but the response terminates at 35%g, below the point of the capacity curve corresponding in Abaqus to the local collapse. In all the cases considered, the presence of the sidewalls is of great importance to improve the structure's stability under vertical and horizontal loading.

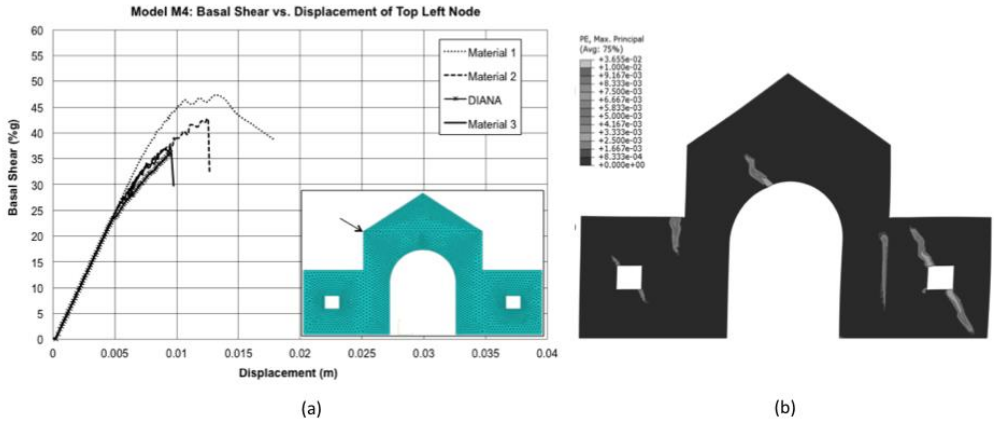

Figure 10 (a) Capacity curves for model M4, and (b) maximum plastic strains at collapse (Abaqus/CAE); displacements are computed at top left corner indicated by arrow in (a)

Model M4: the Arch with Tympanum and Lateral Walls with Window Openings

The capacity curves for Model M4 and the damage status at collapse are illustrated in Figure 10. As for M3, at the end of the gravitational loading no damage is present in the structure, confirming the stabilizing effect of the sidewalls. The similarity with the previous case continues during the initial stages of the horizontal acceleration, as an asymmetric crack develops at the intrados and then turns inward. Thereafter, the pattern changes. For all three materials in Abaqus as well as for Diana, shear fractures originating at the windows quickly develop together with fissures separating the walls from the piers – see Figures 10 (b). Finally, the shear fracture at the right window leads to total collapse of the structure. Materials 1 and 2 yield a capacity of 46%g and 42%g,

respectively, while Material 3 and Diana give the same value of 36%g. In this case too, the increase in compressive fracture energy appears to lower substantially the capacity of the structure.

Models M5 and M6: Variation in the Height of the Sidewalls

Finally, we consider how increasing the height of the lateral walls changes the capacity of the structure, modeled – in this case – with Material 3 only. M5 and M6 denote the wall configurations without and with window openings, respectively. Figure 11 (a) shows the capacity curve for three wall heights: TWH0 (the actual height, same geometry as Model 3), TWH2 (the height of the base of the tympanum), and TWH1 (intermediate between the other two.) As noted earlier in discussing Model 3, TWH0 exhibits a partial collapse at 45%g, due to the detachment of an arch section, followed by total collapse at 56%g. For TWH1 and TWH2 the detachment of the arch section corresponds to the final collapse at 52%g and 47%g, respectively. Therefore, extending the elevation of the lateral walls increases the structural capacity only if we assume the partial collapse of TWH0 as defining the total capacity of the structure in the actual wall configuration. Under the same assumption, extending the elevation increases does not affect the ductility of the structure, which remains at 11 mm.

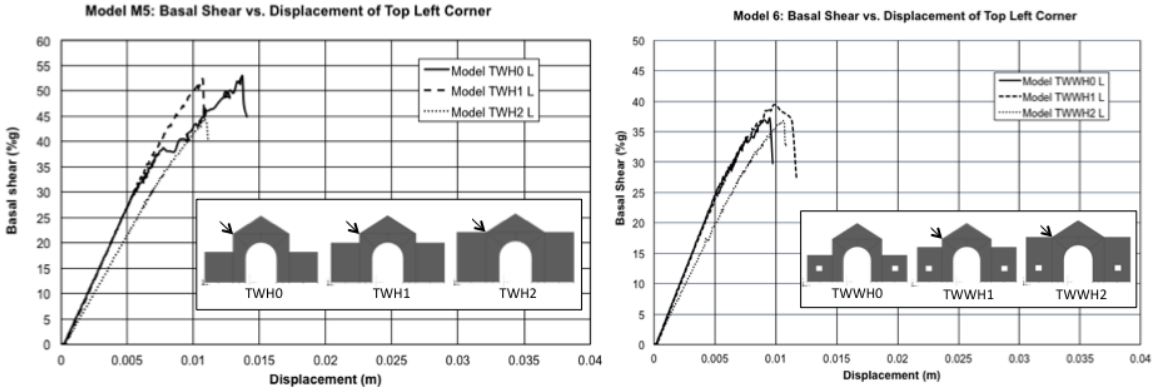

Figure 11 Capacity curves for (a) model M5 and (b) model M6; in each case, three wall heights are considered and the displacements are computed at top left corner indicated by arrow

As shown in Figure 11 (b), when the window openings are taken into account, increasing the wall height has only a marginal effect on the structural capacity – from 37%g to 39%g – as well as the ductility – from 9 mm to 10 mm.

CONCLUSIONS

St. Peter Apostle Church of Andahuaylillas is a representative structure of early colonial Peruvian religious buildings constructed in adobe. Given its remarkable historical, architectural and artistic features, it is considered a masterpiece of the Andean baroque architecture. The seismic assessment of this church requires the individual study of specific structural elements presenting a high damage concentration, as it is the case for the triumphal arch. This paper presents some preliminary results of the seismic evaluation of the arch subjected to in plane lateral accelerations. The study is conducted using similar 2D nonlinear FEM models developed in Abaqus/CAE Explicit and Diana. In order to better understand how each sub-structural element contributes to modulating the capacity of the complete triumphal arch, a sequence of models is constructed by adding to the arch proper first the tympanum and then the lateral walls (with and without window openings.)

The results indicate that the crack pattern and load capacity are substantially affected by the model geometry and by the tensile and compressive fracture energies associated with the material models used to represent the nonlinear behaviour of adobe masonry. The analyses confirm the weakness in tension at or near the centre of the intrados and at the connections with the sidewalls. In general, reducing the tensile fracture energy reduces the structural capacity. However, increasing the compressive fracture energy produces mixed effects: it increases the capacity for M1, but decreases it for all other cases. The latter effect appears to be correlated with the presence of major shear fractures at collapse. On the geometry side, the influence of the shear walls and window openings on the seismic capacity is evident. Shear walls increase considerably the load capacity by stabilizing the arch, but the inclusion of the window openings reduces markedly their effect. Considering the effect of increasing the height of the sidewalls, it appears that the current configurations provides a nearly optimum capacity under the conditions tested with the numerical models.

ACKNOWLEDGMENTS

The authors would like to acknowledge the Pontificia Universidad Católica del Perú and its funding office DGI-PUCP (project 2015-171) for providing funds to the project within which this work was developed. Additional support was provided by the Program in Archaeology, Technology, and Historical Structures of the University of Rochester. Carolina Briceño gratefully acknowledges CONCYTEC for the scholarship in support of postgraduate studies.

REFERENCES

Abaqus CAE (2013). *Software for finite element analysis* Abaqus/Complete Abaqus Environment, Version 6.12. Dassault Systémes. Vélizy-Villacoublay.

Aguilar, R., Ramos, L.F., Torrealva, D., Chácara, C. (2013). "Experimental modal identification of an existent earthen residential building", *In Proc. of the 5th International Operational Modal Analysis Conference (IOMAC 2013)*, Guimaraes, Portugal.

Aguilar, R., Sovero, K., Martel, C., Chácara, C., Boroschek, R. (2013). "Advanced techniques for the seismic protection of existing heritage", *BiT La Revista Técnica de la Construcción*, 90:58-61.

Allemang, J.R. (2003). "*The modal assurance criterion-twenty years of use and abuse. Sound and Vibration*", 37(8):14 23.

Binda, L., Saisi, A. (2001). "State of the art of research on historic structures in Italy". *Research report*: Polytechnic of Milan, Department of Structural Engineering, Milan, Italy.

Castillo, M., Kuon, E., Aguirre, C. (2012). "*Saint Peter the Apostle of Andahuaylillas: tour guide*", Association Jesus Obrero, Cusco, Peru.

De Luca, A., Giordano, A. & Mele, E. (2004). "A simplified procedure for assessing the seismic capacity of masonry arches", *Engineering Structures,* 26 (13), 1915-1929.

Diana (2013). *Displacement method Analyser*, Version 9.4.4. TNO Diana BV. Delft

Fonseca, F., D'Ayala, D. (2012). "Seismic assessment and retrofitting of Peruvian earthen churches by means of numerical modelling", *In Proc. of the 15th World Conference on Earthquake Engineering*, Lisbon, Spain.

Giuffrè, A., Carocci, C. (1996) "Vulnerability and mitigation in historical centers in seismic areas: Criteria for the formulation of a "practice code". *In Proc. of the 11th World Conference on Earthquake Engineering. Elsevier*: Acapulco, Mexico.

Houben, H., Guillaud, H. & Hall, B.B. (1994). "Earth construction: a comprehensive guide", *Intermediate Technology Publications*, London, UK.

Lourenco, P.B. (2009). "Recent advances in masonry structures: Micromodelling and homogenization*". In Multiscale Modeling in Solid Mechanics: Computational Approaches*. ed. U. Galvanetto & M.H. Ferri Aliabadi, Imperial College Press, 251-294, London, UK.

Mele, E., De Luca, A. & Giordano, A. (2003). "Modelling and analysis of a basilica under earthquake loading", *Journal of Cultural Heritage*, 4(4), 355-367.

NTE.010 (2006). "*Reglamento de edificaciones del Perú, Norma técnica E.010: Madera*" (`Peruvian design code for wood structures). SENCICO: Lima, Peru.

Tarque, N., Camata, G., Espacone, E., Varum, H. and Blondet, M. (2010) "Numerical modelling of in-plane behaviour of adobe walls", *8^0 Congresso de Sismologia e Engenharia Sismica (SISMICA 2010)*, Aveiro, Portugal.

Van der Pluijm, R. (1999). "*Out of plane bending of masonry: Behaviour and strength*" PhD thesis, Eindhoven University of Technology: Eindhoven, Netherlands.

Vargas, J., Aguilar, R., Gonzales, M., Briceño, C. (2013). "Structural Intervention in Saint Peter the Apostle Church Of Andahuaylillas in Cusco, Peru", *In Proc. of the 13th Ibero-American Seminar on Earthen Architecture and Construction (XIII SIACOT)*, Valparaiso, Chile.

www.andahuaylillas.com (2015) *Website of the Institutional Social Project in Andahuaylillas*.